Periodica Polytechnica Mechanical Engineering

A New Wireless Modular Device for Rapid Measurements of Structural Motions

Balázs Havasi-Tóth[1,2], Csaba Bagyinszki[1], Balázs Farkas[1*]

[1] Department of Fluid Mechanics, Faculty of Mechanical Engineering, Budapest University of Technology and Economics, Műegyetem rkp. 3., H-1111 Budapest, Hungary
[2] HUN-REN-BME Morphodynamics Research Group, Budapest University of Technology and Economics, Műegyetem rkp. 3., H-1111 Budapest, Hungary
[*] Corresponding author, e-mail: farkas.balazs@gpk.bme.hu

Received: 19 April 2026, Accepted: 18 July 2026, Published online: 14 August 2026

Abstract

In this paper, we present an internally developed sensing system featuring an integrated 6-axis inertial measurement unit designed to provide a rapid and remarkably simple solution for measuring low frequency vibrations – such as flow-induced vibrations – or other movements of solid structures in educational, research, and industrial applications. Given its highly compact form factor, the device supports wireless communication and onboard data logging to a memory card. Since neither power supply nor data transmission requires a wired connection, it is also suitable for analysing the motion of untethered, freely moving bodies. According to its modular architecture, the sensor can be fitted with custom housings tailored to diverse geometric constraints and produced rapidly using SLA 3D printing technology. In addition to outlining the design considerations, we detail the device's construction and capabilities, then validate its performance by comparing measurement results from a simple autonomous chaotic mechanical system experiment with a vision-based measurement method.

Keywords

portable accelerometer, experimental, structural motion, SLA printed housing

1 Introduction

The necessity of developing accurate accelerometers is underscored by their critical role in capturing dynamic data within fluid-mechanics-related research. In sports biomechanics, for instance, evaluating the effect of finger spread on swimmer performance requires the precise mapping of stroke trajectories [1]. Wearable accelerometers have emerged as a viable alternative for this task, proving effective and reliable when compared to traditional image-processed data, which often suffers from parallax errors and occlusion under water [2].

Accelerometers can also be applied effectively in atmospheric research. While the study of atmospheric flows has historically been hindered by a deficiency in experimental data, simple yet robust sensors attached to meteorological balloons now provide vital insights into turbulent behaviour at high altitudes [3]. This demand for high-fidelity data extends into structural engineering and aviation, where determining the flutter behaviour of flexible structures – such as suspension bridges and aircraft – is crucial for operational safety. In flight testing, wing-mounted accelerometers are the standard for identifying critical flutter speeds, providing the essential data needed to prevent catastrophic structural failure [4]. Similarly, in maritime environments, buoy-mounted accelerometers provide critical data on wave-induced motion, essential for both oceanographic monitoring [5] and the validation of numerical models for floating body investigations [6].

Another noteworthy application with geomorphological implications is the investigation of the behaviour and typical movement of sedimentary particles driven by fluvial or coastal currents, depending on the flow conditions. The significance of this lies in gaining a deeper understanding of bed erosion and the morphological evolution of pebbles through abrasion. Numerous geomorphological studies have addressed the movement of pebbles placed in currents [7–9], cases in which accelerometers can be utilized highly

Cite this article as: Havasi-Tóth, B., Bagyinszki, C., Farkas, B. "A New Wireless Modular Device for Rapid Measurements of Structural Motions", Periodica Polytechnica Mechanical Engineering, 2026. https://doi.org/10.3311/PPme.44387

effectively. Although dedicated devices have been developed for this purpose in the past [10–13], the general applicability of these accelerometers remains significantly limited.

Despite the diversity of these fields, they share a common challenge: the requirement for high-resolution data collection without altering the physical properties of the subject. In fluid-dynamic environments, the presence of a sensor itself can become a source of error, either through its physical mass or the aerodynamic disturbance of its mounting.

While a vast array of accelerometers is available on the market, existing solutions often fail to meet the specialized requirements of high-precision research, particularly regarding cost-effectiveness and seamless integration. Critical features such as a modular design and ultra-compact form factor are rarely found in off-the-shelf products. These characteristics are essential for minimizing the 'added mass' effect on sensitive structures, such as a swimmer's fingers or lightweight aircraft wings, where even a few grams of additional weight can shift the behaviour of the system. Furthermore, wireless architecture is imperative; eliminating cabling not only removes mechanical constraints on motion but also prevents aerodynamic interference that could trip laminar flows into turbulence.

Consequently, our objective was to design and manufacture a versatile, low-cost device that bridges the gap between educational accessibility, academic research, and industrial measurement applications. By prioritizing a "minimally invasive" design philosophy, this device seeks to provide a scalable solution for multi-point sensing in environments where traditional instrumentation remains too bulky or cost-prohibitive.

2 Design of the modular device

2.1 Motivation and objectives

Before starting the development, our requirements for the accelerometer were synthesized into the following specifications:

- 6-axis inertial measurement unit: (accelerations and angular velocities along the x, y, and z axes),
- High-speed wireless communication: enabling limited sampling frequency real-time data transmission for real-time monitoring purposes,
- Modular architecture: allowing the sensor to be fitted with any custom built housing,
- Ultra-compact form factor: achieving the smallest possible size within rational constraints,
- Flexible power management: compatibility with batteries of various sizes and capacities depending on the application, entirely eliminating the need for external power supplies or data cables,
- Integrated microSD slot: providing high-frequency data logging (at sampling rates exceeding those of wireless transmission),
- Optimized performance: achieving the highest possible sampling frequencies and acceleration ranges while fulfilling all the above requirements.

In addition to the requirements listed above, we prioritized ease of manufacture, the use of widely available off-the-shelf components, and the minimization of per-unit production costs.

Leveraging recently available high-precision SLA 3D printing techniques, which is capable of providing excellent mechanical properties, our custom-designed accelerometer can be fitted with a housing of almost any shape. This flexibility facilitates seamless integration, even under the most diverse geometric constraints.

2.2 Considerations and technical data

The device was uniquely designed at the Department of Fluid Mechanics at the Budapest University of Technology and Economics for studying the flow-induced motion and interaction of different solid structures, primarily in laboratory environment. The need for a custom solution stems from the specific combination of requirements set by the planned applications. Therefore, the development was an iterative process during which the main objective was to make the device as small as possible – without losing functionality – to be able to cover the widest possible range of applications. The drawing of the final version of the device with the dimensions is shown by Fig. 1.

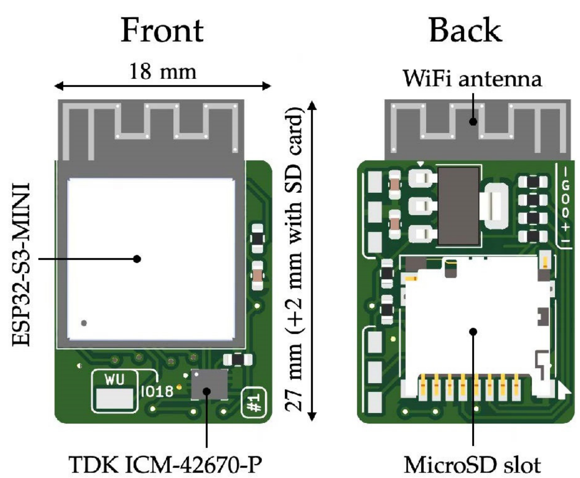

Fig. 1 Front and back views of the final design of the board. The thickness of the board without the battery is 5.8 mm.

It must be noted that the dimensions (18 × 29 × 5.8 mm) do not include the power supply, as it might depend on the specific case (in terms of available space and targeted measurement duration) the device is used for.

The device is designed around the ESP32-S3-MINI-1-N8 module, which was selected for its excellent computational and wireless communication capabilities. The sensor used for tracking motions is the TDK ICM-42670-P 6-axis (three acceleration and three angular velocity components) inertial measurement unit, which provides accurate measurements in a wide range for a low cost. Since the ESP32-S3-MINI-1-N8 module operates from 3.3 volts (and tolerates input voltages between 3 and 3.6 volts), and a single-cell LiPo battery provides between 3.2 and 4.2 volts (depending on charge level), a voltage regulator module is used to ensure proper operation and avoid potential hardware damages. For this purpose, the MCP1826S-3302E/DB was selected, as it covers the entire usable range of our battery and has a fixed output of 3.3 volts. The maximum output current of the voltage regulator is 1 A. Based on our experiences, the device has a current consumption of slightly over 100 mA in the relevant applications, so using the above-mentioned voltage regulator is a deliberate oversizing from our part to account for possible consumption spikes (up to around 500 mA) and avoid excessive heating. The microSD module is of type DM3D-SF, which was selected for its low space requirements and cost. The passive elements are all of the standardized package size of 1608 (0603 in imperial), resulting in a small size while not sacrificing the possibility of manual assembly and repair. The overall characteristics of the device resulting from the properties of the used components are presented in Table 1 [14].

Table 1 Summary listing of the device properties [14]

Property	Value	Unit
Length	29	mm
Width	18	mm
Thickness	5.8	mm
Maximum CPU frequency	240	MHz
Accel. measurement limit	±160	m/s^2
Gyroscope measurement limit	±2000	°/s
Input voltage	2.3...6	V
Operating temperature	−10...45	°C
Acceleration uncertainty	±1	%
Acceleration rest offset	0.4	m/s^2
Gyroscope uncertainty	±1	%
Gyroscope rest offset	±1	°/s

Although high-frequency data logging occurs on the microSD card, wireless data transmission of a lower frequency is implemented to be able to monitor the measurement real-time. For this purpose, the built-in antenna of the ESP32-S3-MINI-1-N8 is used to eliminate the need for designing an additional impedance-matching circuit. The wireless communication between the device and a computer is realized using 2.4 GHz Wi-Fi connection. Despite the limited penetration depth of these frequencies in water, underwater experiments were successfully conducted using a 3D-printed, hermetically sealed housing. Again, the absence of power and data cables significantly simplified the waterproofing process. It should be noted that while a connection loss terminates real-time monitoring, data logging continues uninterrupted on the local SD card.

Due to its even further reduced size, the device lacks built-in data ports. Initial firmware is uploaded by soldering a standard USB data cable directly to the board, which can then be removed. To eliminate the need for repeated manual soldering, all subsequent updates are performed wirelessly via OTA (over-the-air) firmware updates.

3 Verification of the device operation

3.1 The accelerometer unit

The most beneficial features of the accelerometer are its compact size, lightweight design, and the fact that it enables wireless operation. Consequently, the motion of almost any structure involving large displacements can be investigated without significantly influencing the system. Taking these factors into account, this chapter presents the application of the accelerometer through a laboratory experiment.

In our measurements, we used a regular 32 GB microSD card and the commercially available 70 single-cell lithium-ion polymer (LiPo) battery (dimensions: 15 × 15 × 5 mm without the cables and connector) manufactured by TinyCircuits providing ~25 minutes of continuous operation in the worst case with simultaneous wireless data transfer enabled, which accounts for by far the largest share of power consumption. The complete set of components and the assembled accelerometer is presented in Fig. 2. Note, that the SLA-printed housing was built for the present exact purpose and due to the modular design, it can be arbitrarily changed according to the application environment. Including the housing, the total weight of the device is 14.5 g (accelerometer: 4.5 g, battery: 2 g, housing: 8 g).

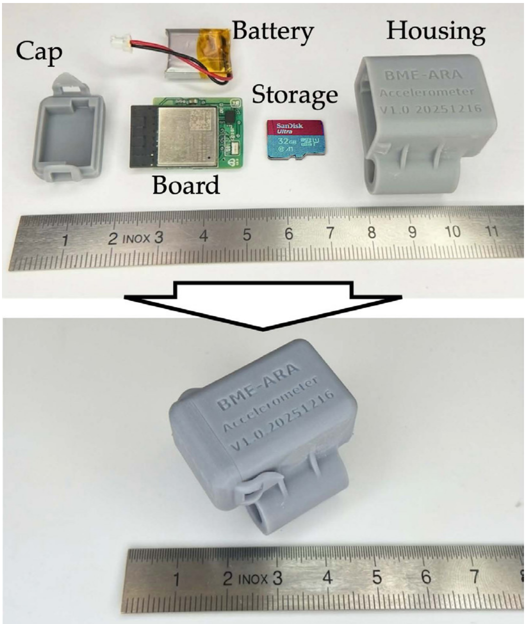

Fig. 2 Top: the board, microSD card, battery and the 3D printed housing. Bottom: the assembled accelerometer.

3.2 The experimental setup and results

Keeping the simplicity of the test case in mind, the motion of a double pendulum is measured both visually and, simultaneously, using the accelerometer. The experimental layout is shown in Fig. 3 with the markers facilitating the visual tracking of the motion. The length of both arms of the pendulum is 200 mm. We chose concentric circular markers so that the tracking becomes insensitive to rotation of the arms. Since the instantaneous locations of the markers were determined via cross-correlation in each image frame, their different radii prevent misidentification, even with grayscale image processing. With the accurately detected positions of the two markers, the instantaneous alignment of the two Degree of Freedom pendulum can be uniquely determined.

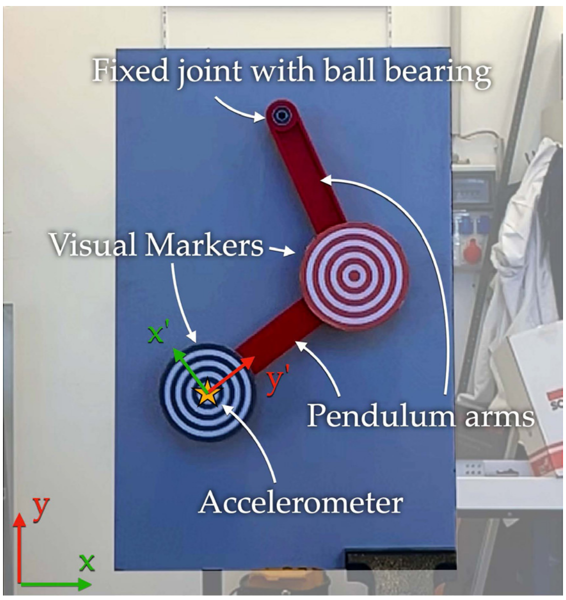

Fig. 3 Instantaneous layout of the double pendulum with the visual markers and the accelerometer at the tip of the lower arm. The colored arrows show the global and the accelerometer's local coordinate system.

We carried out three measurements of the pendulum motion for 10 seconds each with different initial conditions using a 240 fps (frames per second) camera of an Iphone 13 smartphone [15], and 1 kHz sampling frequency of the accelerometer. While the accelerometer is fixed at the tip of the rotating lower arm, the sensor's local coordinate system is inherently different from that of the visual reconstruction. Furthermore, the output values provided by the two measurement procedures (positions from the visual measurement; accelerations and angular velocities from the accelerometer) are not directly comparable. Therefore, our goal was to convert the visual data to the accelerometer's frame. After each measurement, the conversion was carried out by a workflow containing the following steps on order:

1. Filtering of the raw position data: Following the experiments, the time series of the positions of the markers mounted on the tips of the pendulum arms were determined using frame-by-frame cross-correlation computed from the marker images within the visual dataset using Matlab 2024b [16]. In order for the position data to be numerically differentiated without amplifying the inherent noise of the visual reconstruction, we applied a moving average filter with a window size of 0.02 s on the raw data. The window size was chosen so that the relevant components of the relatively slow motion were accurately preserved. The angular velocity time series of the lower arm were computed from the first derivative of the filtered position data. No filtering was applied on the accelerometer's data.
2. Differentiation of the filtered data twice to obtain acceleration data in the global frame of the visual experiments. The second time derivative was determined using a second-order central differencing scheme.
3. Transformation of the obtained data to the accelerometer's frame of reference. Knowing the instantaneous pendulum angles (cf. markers' positions), the deduced acceleration data were transformed to the accelerometer's coordinate system with the transformation given as

$$\boldsymbol{a}'_v = \begin{bmatrix} -e'_y & e'_x \\ e'_x & e'_y \end{bmatrix} \cdot \left(\boldsymbol{a}_v + \boldsymbol{g}\right), \tag{1}$$

where e'_x and e'_y are the basis vectors of the accelerometer's instantaneous local coordinate system shown in Fig. 3 and $\boldsymbol{g} = [0 - 9.81]$ m/s^2. Accounting for gravitational acceleration is necessary because the accelerometer measurements continuously capture gravitational acceleration as well, whereas the visual measurement does not record any regarding information.

Since the accelerometer behaves as a passive element from the perspective of the dynamical system during the measurement – that is, there is no closed-loop control in the system – we neglected the time delay of the accelerometer. The temporal synchronization between the camera and the accelerometer was also performed via cross-correlation, following the transformation of the visual measurement data according to Eq. (1). Thus, the direct comparison became achievable utilizing the corresponding timestamps and a linear interpolation between the data series of different sampling frequencies.

After performing the evaluation steps 1–3, Fig. 4 presents the comparison between the 1000 Hz datasets recorded by the accelerometer and the 240 Hz data derived from the visual measurement. According to the diagrams, the time series show a good qualitative and quantitative agreement in case of both the accelerometer and gyroscope measurements. The root mean square errors

$$RMSE_a = \sqrt{\sum_{i=1}^{N} \frac{\left(\left| \boldsymbol{a}'_v \right|_i - \left| \boldsymbol{a}'_a \right|_i \right)^2}{N}},$$
$$RMSE_\omega = \sqrt{\sum_{i=1}^{N} \frac{\left(\omega_{v_i} - \omega_{v_i} \right)^2}{N}} \quad (2)$$

of the acceleration and measurement data are listed in Table 2. Here, N is the number of timestamps, and the lower indices v and a refer to visual and accelerometer data.

4 Discussion on future developments and applications

In this study, our objective was to develop a highly compact, general-purpose, modular wireless accelerometer suitable for effective application in engineering such as the experimental investigation of wind-induced vibrations and other fields including geomorphology. Following its construction, the device was equipped with a protective casing produced via SLA (stereolithography) 3D printing, which also facilitates mounting. This casing can be freely modified or replaced depending on the specific application, the installation environment, and the size of the battery. Due to its wireless design, the device is also suitable for underwater experiments when fitted with a waterproof

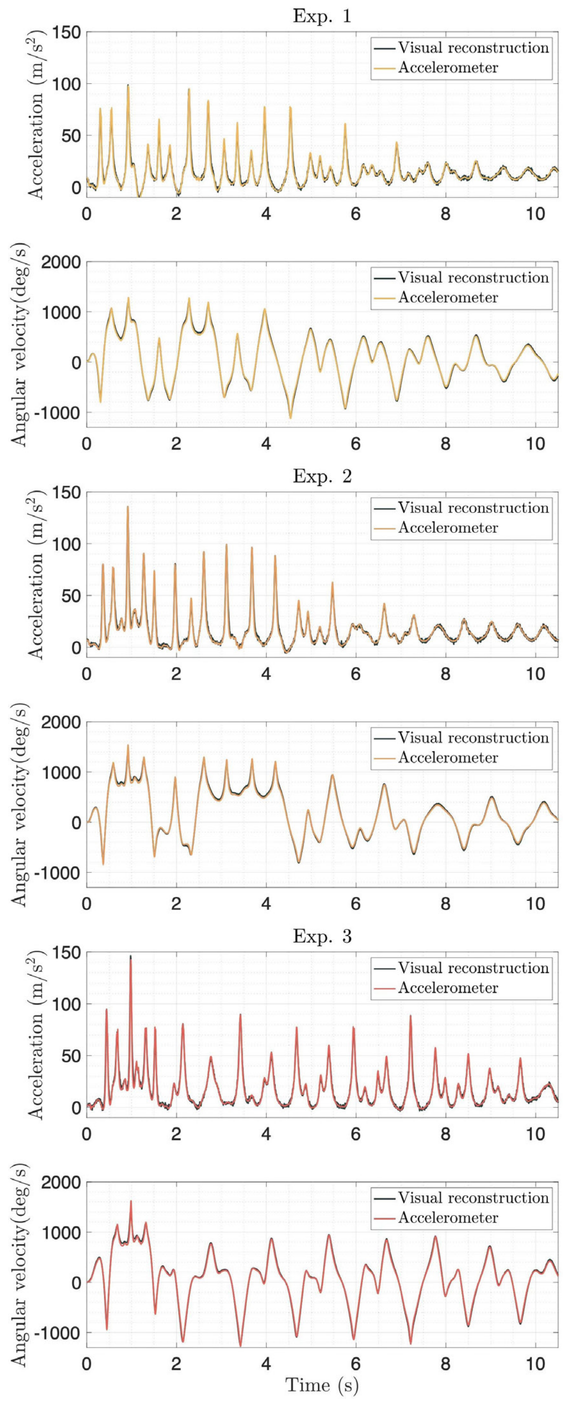

Fig. 4 Comparison of the three experimental data (Exp. 1...3) acquired using the accelerometer and the visual reconstruction. Acceleration's y' is plotted in time with the angular velocity perpendicular to the pendulum's plane.

Table 2 Acceleration ($RMSE_a$) and angular velocity ($RMSE_\omega$) root mean square error values of the three experiments

	$RMSE_a$ (m/s^2)	$RMSE_\omega$ (deg/s)
Exp. 1	2.35	33.03
Exp. 2	2.11	28.87
Exp. 3	2.03	29.20

enclosure. In the near future, utilizing its key features, we will employ the device in a freely moving wireless smart pebble to investigate typical rolling and saltating motion of sedimentary particles. We also plan to integrate a Hall sensor, which will allow for contactless switching of the device without the need to repeatedly disassemble and reassemble the housing. In such cases, while real-time wireless data transmission may present challenges due to the underwater operation, it does not affect the recording of acceleration and angular velocity data to local storage. As a further development, Kalman filters can be implemented to reconstruct the motion of pebbles or more complex dynamic systems, adapting the post-processing to the requirements of the desired application.

References

[1] Farkas, B., Suda, J. M. "Experimental and Numerical Investigation on the Effect of Finger Spread on Swimmer Performance", Periodica Polytechnica Mechanical Engineering, 69(3), pp. 234–241, 2025. https://doi.org/10.3311/PPme.40916

[2] Callaway, A. J., Cobb, J. E., Jones, I. "A Comparison of Video and Accelerometer Based Approaches Applied to Performance Monitoring in Swimming", International Journal of Sports Science & Coaching, 4(1), pp. 139–153, 2009. https://doi.org/10.1260/1747-9541.4.1.139

[3] Marlton, G. J., Harrison, R. G., Nicoll, K. A., Williams, P. D. "Note: A balloon-borne accelerometer technique for measuring atmospheric turbulence", Review of Scientific Instruments, 86(1), 016109, 2015. https://doi.org/10.1063/1.4905529

[4] Soal, K. I., Schwochow, J., Volkmar, R., Tang, M., Thiem, C., Govers, Y., ..., Nagy, M. "Flutter flight testing: Using operational modal analysis to identify, track and predict flutter for safe and efficient flight test campaigns", In: International Forum on Aeroelasticity and Structural Dynamics IFASD 2024, Hague, Netherlands, 2024. Available at: https://conf.ifasd2024.nl/proceedings/display_manuscript/119.htm [Accessed: 16 July 2026]

[5] Benetazzo, A., Bergamasco, F., Barbariol, F., Ferla, M., Nardone, G., …, Cavaleri L. "Evaluation of the 3D response and performance of an operational wave buoy for coastal wave monitoring", Coastal Engineering, 200, 104756, 2025. https://doi.org/10.1016/j.coastaleng.2025.104756

[6] Havasi-Tóth, B., Farkas, B. "Reconstruction of 3D Floating Body Motion on Shallow WaterFlows Using the Smoothed Particle Hydrodynamics Method", Periodica Polytechnica Mechanical Engineering, 70(1), pp. 51–58, 2026. https://doi.org/10.3311/PPme.42722

[7] Becker, K., Gronz, O., Wirtz, S., Seeger, M., Brings, C., Iserloh, T., Casper, M. C., Ries, J. B. "Characterization of complex pebble movement patterns in channel flow–a laboratory study", Cuadernos de Investigación Geográfica: Geographical Research Letters, 41(1), pp. 63–85. 2015. Available at: https://dialnet.unirioja.es/servlet/articulo?codigo=5102744 [Accessed: 16 July 2026]

[8] Cassel, M., Lavé, J., Recking, A., Malavoi, J.-R., Piégay, H. "Bedload transport in rivers, size matters but so does shape", Scientific Reports, 11(1), 508, 2021. https://doi.org/10.1038/s41598-020-79930-7

[9] Winzer, K. "Hopping of elliptical pebbles on the beach and laboratory results", The European Physical Journal Plus, 138(7), 596, 2023. https://doi.org/10.1140/epjp/s13360-023-04140-9

[10] Akeila, E., Salcic, Z., Swain, A. "Smart Pebble for Monitoring Riverbed Sediment Transport", IEEE Sensors Journal, (10)11, pp. 1705–1717, 2010. https://doi.org/10.1109/JSEN.2010.2046726

[11] Yuan, J., Wang, P., Wang, M., Wang, M. "Experimental Investigations on the Response of Bedload Sediment to Vibration", Sustainability, 15(15), 11972. 2023. https://doi.org/10.3390/su151511972

[12] Husain, S. F., Abbas, M. S., Wang, H., Qamhia, I. I., Tutumluer, E., Wallace, J., Hammond, M. "A laboratory-scale evaluation of smart pebble sensors embedded in geomaterials", Sensors, 24(9), 2733, 2024. https://doi.org/10.3390/s24092733

[13] Xie, Y., Melville, B. W., Shamseldin, A. Y., Whittaker, C. N., Yang, Y. "Smart Sediment Particle: A novel approach to investigating fluvial bed entrainment using instrumented sensors", International Journal of Sediment Research, 38(1), pp. 66–82, 2023. https://doi.org/10.1016/j.ijsrc.2022.08.003

[14] TDK InvenSense "ICM-42670-P Datasheet" [online] Available at: https://product.tdk.com/system/files/dam/doc/product/sensor/mortion-inertial/imu/data_sheet/ds-000451-icm-42670-p.pdf [Accessed: 16 July 2026]

[15] Apple Inc. "iPhone 13 - Tech Specs" [online] Available at: https://support.apple.com/en-us/111872 [Accessed: 16 July 2026]

[16] The Mathworks, Inc. "Matlab", [computer program] Available at: https://uk.mathworks.com/products/matlab.html [Accessed: 16 July 2026]